Article

Cell Reports

A Polyadenylation-Dependent 3′ End Maturation Pathway Is Required for the Synthesis of the Human Telomerase RNA

Graphical Abstract

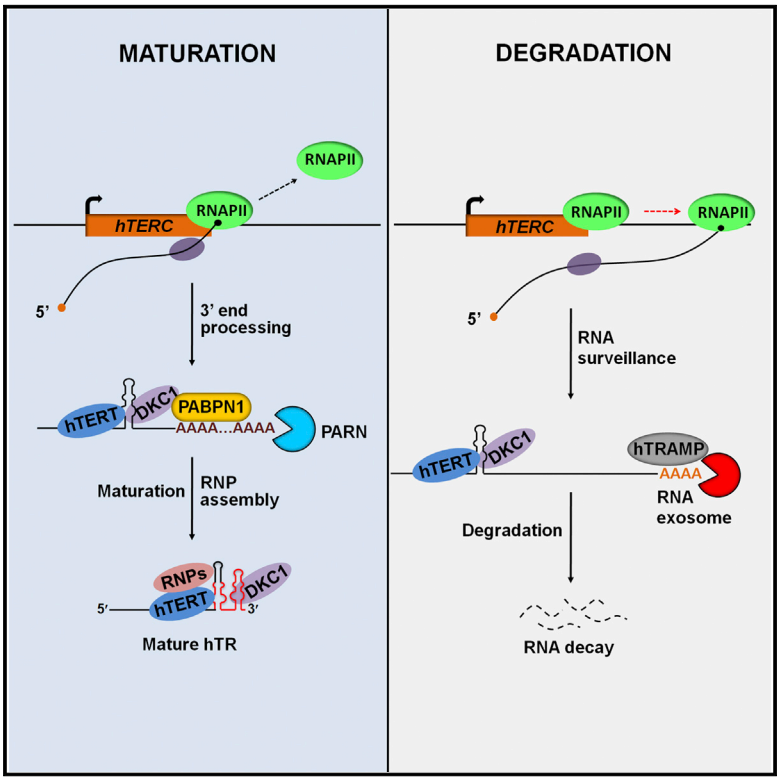

Highlights

- Maturation of human telomerase RNA requires 3′ end polyadenylation
- PABPN1 and PARN promote poly(A)-dependent telomerase RNA 3′ end maturation
- The RNA exosome functions in telomerase RNP surveillance
- The equilibrium between decay and maturation controls telomerase RNA accumulation

Authors

Duy Nguyen, Valérie Grenier St-Sauveur, Danny Bergeron, Fabien Dupuis-Sandoval, Michelle S. Scott, François Bachand

Correspondence

f.bachand@usherbrooke.ca

In Brief

Nguyen et al. present evidence that the functional, non-polyadenylated human telomerase RNA is matured via a 3′ end polyadenylation step that requires the poly(A)-specific factors PABPN1 and PARN. Their findings unveil a critical requirement for RNA polyadenylation in telomerase RNA biogenesis, providing alternative approaches for telomerase inhibition in cancer.

Accession Numbers

GSE74186

Nguyen et al., 2015, Cell Reports *13*, 2244–2257
December 15, 2015
http://dx.doi.org/10.1016/j.celrep.2015.11.003

OPEN ACCESS
CellPress

Cell Reports
Article

A Polyadenylation-Dependent 3′ End Maturation Pathway Is Required for the Synthesis of the Human Telomerase RNA

Duy Nguyen,[1] Valérie Grenier St-Sauveur,[1] Danny Bergeron,[1] Fabien Dupuis-Sandoval,[1] Michelle S. Scott,[1] and François Bachand[1,*]
[1]RNA Group, Department of Biochemistry, Université de Sherbrooke, Sherbrooke, QC J1E 4K8, Canada
*Correspondence: f.bachand@usherbrooke.ca
http://dx.doi.org/10.1016/j.celrep.2015.11.003

SUMMARY

Telomere maintenance by the telomerase reverse transcriptase requires a noncoding RNA subunit that acts as a template for the synthesis of telomeric repeats. In humans, the telomerase RNA (hTR) is a non-polyadenylated transcript produced from an independent transcriptional unit. As yet, the mechanism and factors responsible for hTR 3′ end processing have remained largely unknown. Here, we show that hTR is matured via a polyadenylation-dependent pathway that relies on the nuclear poly(A)-binding protein PABPN1 and the poly(A)-specific RNase PARN. Depletion of PABPN1 and PARN results in telomerase RNA deficiency and the accumulation of polyadenylated precursors. Accordingly, a deficiency in PABPN1 leads to impaired telomerase activity and telomere shortening. In contrast, we find that hTRAMP-dependent polyadenylation and exosome-mediated degradation function antagonistically to hTR maturation, thereby limiting telomerase RNA accumulation. Our findings unveil a critical requirement for RNA polyadenylation in telomerase RNA biogenesis, providing alternative approaches for telomerase inhibition in cancer.

INTRODUCTION

In most eukaryotes, the ends of chromosomes (telomeres) cannot be fully duplicated as a consequence of incomplete replication of the lagging strand by the conventional DNA replication machinery. To cope with this end-replication problem, many species use a specialized ribonucleoprotein (RNP) complex with reverse transcriptase activity, known as telomerase, to synthesize tandem DNA repeats at chromosomal ends. Accordingly, telomeric DNA progressively shortens after each cell division in the absence of telomerase, ultimately causing the collapse of the DNA-protein structure that caps chromosome ends and the activation of DNA damage checkpoints (Webb et al., 2013). Such checkpoints ultimately lead to growth arrest via the activation of cellular senescence or apoptosis pathways (Artandi and DePinho, 2010). Because critically short telomeres lead to terminal cell-cycle arrest, human telomerase is strongly associated with cellular immortalization and tumorigenesis. Specifically, whereas a vast majority of human somatic cells exhibit low or undetectable levels of telomerase activity, telomerase is active in most human cancers (Kim et al., 1994).

Human telomerase activity can be reconstituted in vitro (Beattie et al., 1998) by the minimal combination of the human telomerase reverse transcriptase (hTERT) and the human telomerase RNA (hTR), which serves as a template for the reverse transcription reaction. In vivo, however, biogenesis of the telomerase holoenzyme requires a variety of interacting partners that play important roles in assembly, maturation, localization, and stabilization of the telomerase complex (Egan and Collins, 2012). In contrast to the telomerase catalytic subunit, which is highly conserved, the noncoding RNA subunit of telomerase is remarkably divergent among eukaryotic species, varying in nucleotide sequences and length (Egan and Collins, 2012). In humans, hTR is a 451-nt-long non-polyadenylated RNA transcribed by RNA polymerase II (Pol II). In addition to a template region that serves in the synthesis of telomeric repeats, vertebrate telomerase RNAs contain a box H/ACA domain at their 3′ end, which is not required for telomerase activity in vitro (Bachand and Autexier, 2001) but for RNA accumulation in vivo (Mitchell et al., 1999a). The box H/ACA motif is an evolutionarily conserved region found in small nucleolar RNAs (snoRNAs) and small Cajal body-specific RNAs (scaRNAs) that serve as guide for the pseudouridylation of rRNAs and spliceosomal small nuclear RNAs (snRNAs), respectively (Kiss et al., 2010). As for H/ACA RNPs, the box H/ACA domain of hTR folds into a structure recognized by a set of evolutionarily conserved proteins, including Dyskerin, Nop10, Nhp2, and Gar1 (Egan and Collins, 2012). Accordingly, a deficiency in any of these proteins results in reduced levels of telomerase RNA and shorter telomeres (Mitchell et al., 1999b; Vulliamy et al., 2008). Despite the presence of a snoRNA-like H/ACA box at its 3′ end, hTR synthesis contrasts to most mammalian snoRNA genes. Indeed, whereas the majority of human snoRNAs are expressed as part of pre-mRNA introns and processed from intron lariats into mature

snoRNAs (Dieci et al., 2009), hTR is expressed from an independent transcriptional unit. However, the RNA-processing pathway involved in the 3′ end maturation of hTR remains poorly understood.

In contrast to humans, most yeast snoRNAs are synthesized from independent transcriptional units using factors and pathways that have been relatively well characterized. Specifically, yeast snoRNAs are matured via two alternative pathways: a mechanism that depends on the activity of the Nrd1-Nab3-Sen1 (NNS) complex and another that is independent of the NNS complex. In *S. cerevisiae*, the NNS complex promotes a transcription termination pathway that involves recruitment of TRAMP, a nuclear polyadenylation complex that includes the non-canonical poly(A) polymerases (PAPs) Trf4/5, the RNA-binding proteins Air1/2, and the RNA helicase Mtr4 (Porrua and Libri, 2015). By adding short oligo(A) tails, the TRAMP complex provides an unstructured extension to the 3′ end of RNAs, which promotes processing or degradation by the RNA exosome (Schmidt and Butler, 2013). The exosome consists of a barrel-like structure that contains ten core subunits, including the 3′–5′ exonuclease and endonuclease Dis3/Rrp44 (Chlebowski et al., 2013). In the nucleus, the core exosome also associates with an additional 3′–5′ exonuclease, Rrp6, which has redundant and complementary functions to Dis3. Thus, termination of transcription by the NNS complex can promote 3′ end trimming of snoRNAs by the exosome (Tudek et al., 2014). Alternatively, we and others have shown that yeast snoRNAs also can be matured via a polyadenylation-dependent pathway that involves the canonical mRNA 3′ end processing machinery (Grzechnik and Kufel, 2008; Lemay et al., 2010). In the fission yeast *S. pombe*, this maturation pathway involves polyadenylation of 3′-extended precursors by the canonical PAP and 3′ end maturation via the activity of a nuclear poly(A)-binding protein, Pab2, and the exonucleolytic activity of Rrp6. Accordingly, *S. pombe pab2* mutants accumulate polyadenylated snoRNA precursors, whereas levels of mature box H/ACA snoRNAs are reduced (Lemay et al., 2010). Interestingly, the homolog of *S. pombe* Pab2, PABPN1, also has been shown to promote RNA turnover in human cells (Beaulieu et al., 2012; Bresson and Conrad, 2013).

Given that NNS-like transcription termination does not appear to be conserved in mammalian cells (Porrua and Libri, 2015), it remains unclear how independently transcribed human snoRNAs, such as hTR, acquire their mature 3′ end. In this study, we found a polyadenylation-dependent 3′ end maturation pathway for the human telomerase RNA that relies on the nuclear poly(A)-binding protein PABPN1 and the poly(A)-specific RNase PARN. We demonstrated that PABPN1 is bound to polyadenylated telomerase RNA precursors and copurifies with hTERT and Dyskerin. PABPN1-deficient cells showed reduced levels of hTR, exhibited decreased levels of telomerase activity, and had shorter telomeres. In contrast, we found that cells deficient for the RNA exosome and the human TRAMP polyadenylation complex have increased levels of hTR. Our findings suggest that PABPN1/PARN-dependent maturation and hTRAMP/exosome-dependent RNA decay compete for telomerase RNA precursors and that the equilibrium between decay and maturation of precursors controls hTR expression.

RESULTS

PABPN1 Is Required for hTR Accumulation and Telomere Maintenance

To test whether the human homolog of *S. pombe* Pab2, PABPN1, functions in the maturation of H/ACA snoRNAs expressed from independent transcription units, we analyzed hTR, as the *hTR* gene is independently transcribed by Pol II and the resulting RNA processed as an H/ACA box RNA (Mitchell et al., 1999a). PABPN1 was efficiently depleted from HeLa cells using a set of independent small interfering RNAs (siRNAs) (Figure 1A, lanes 2 and 3). We next compared hTR levels between PABPN1-depleted and control cells by northern analysis. The levels of hTR were reduced in PABPN1-deficient cells relative to cells treated with a control siRNA (Figure 1B, compare lanes 2 and 3 to lane 1). Similar results were obtained by knocking down PABPN1 expression in HEK293 cells (Figures S1A and S1B). Quantification of northern data from independent depletion experiments revealed a 20%–38% reduction in hTR levels in cells deficient for PABPN1 (Figure 1C). Given that hTR levels were reduced in PABPN1-depleted cells, we next examined whether human telomerase activity was affected. Extracts prepared from HEK293 and HeLa cells that were previously treated with PABPN1-specific and control siRNAs were analyzed by the telomerase repeat amplification protocol (TRAP). Telomerase activity was significantly reduced in PABPN1-deficient cells (Figure 1D, lanes 2, 3, 5, and 6; quantification shown in Figure 1E), consistent with reduced levels of telomerase RNA. From these results, we conclude that PABPN1 is required for the accumulation of hTR in human cells.

To examine the functional consequence of declining hTR levels (and telomerase activity) in PABPN1-deficient cells, we examined telomere length maintenance using a conditional HEK293 cell line that induces PABPN1-specific small hairpin RNAs (shRNAs) under the control of the tetracycline promoter. Addition of the tetracycline derivative, doxycycline, to the culture media resulted in efficient depletion of PABPN1, reduced hTR levels, and decreased telomerase activity (Figures S1A–S1C). We next analyzed telomere dynamics using cells expressing PABPN1-specific and control shRNAs during serial passages in doxycycline-supplemented media. As can be seen in Figure 1F, cells expressing PABPN1-specific shRNAs led to progressive telomere shortening as compared to cells that expressed a non-specific control shRNA (compare lanes 7–12 to lanes 1–6). An unbiased analysis of mean telomere length using a recently described quantitative program that takes into account signal intensity relative to telomere restriction fragment (TRF) length (Göhring et al., 2014) revealed gradual telomere shortening in PABPN1-deficient cells, but not in control cells (Figure S1D). The stabilization in telomere shortening observed after ~60 cell doublings (Figures 1F and S1D) is likely the result of residual PABPN1 levels remaining after doxycycline treatment (Figure S1A, lane 4). Together, these results indicate that PABPN1 is required for telomere length maintenance in telomerase-positive human cancer cells.

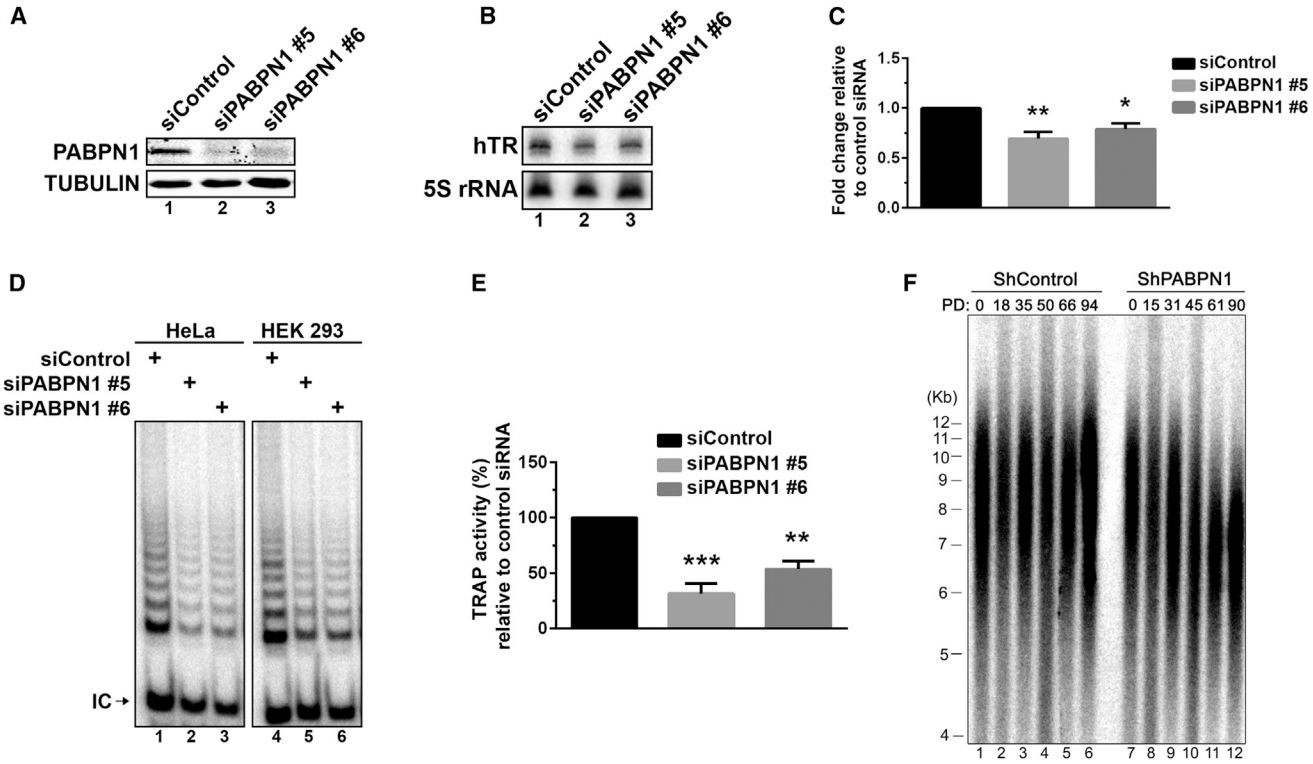

Figure 1. PABPN1 Is Required for hTR Accumulation and Telomere Maintenance

(A) Western analysis of extracts prepared from HeLa cells treated with PABPN1-specific and control siRNAs is shown.

(B) Northern blot analysis of hTR using total RNA prepared from PABPN1-depleted and control cells. The 5S rRNA was used as a loading control.

(C) The hTR levels were normalized to the 5S rRNA and expressed relative to cells treated with control siRNA. Data and error bars represent the mean and SD from four independent experiments (**$p < 0.01$ and *$p < 0.05$, Student's t test).

(D) TRAP assays used extracts prepared from HeLa (lanes 1–3) and HEK293 (lanes 4–6) cells that were previously treated with PABPN1-specific and control siRNAs. IC, internal PCR control.

(E) Quantification of telomerase activity from HeLa cells. The intensity of telomerase products was normalized to the intensity of the IC and expressed relative to cells treated with control siRNA. Data and error bars represent the mean and SD from three independent experiments (***$p < 0.001$ and **$p < 0.01$, Student's t test).

(F) HEK293 cells induced to express PABPN1-specific and non-specific control shRNAs were collected at the indicated population doublings (PDs) and analyzed for telomere length.

See also Figure S1.

PABPN1-Deficient Cells Accumulate 3′-Extended Polyadenylated Telomerase RNA

The reduction of mature snoRNA levels detected in *S. pombe pab2* mutants is associated with the accumulation of 3′-extended snoRNAs (Lemay et al., 2010). We therefore examined PABPN1-depleted cells for the accumulation of 3′-extended human telomerase RNA. Total RNA was extracted from cells treated with PABPN1-specific and control siRNAs and analyzed by RT-PCR using a forward primer positioned in hTR (Figure 2A, see primer F2) and reverse primers positioned 159- and 445-nt downstream of the 3′ end of mature hTR (Figure 2A, see R1 and R2 primers, respectively). RT-PCR analysis detected increased levels of 3′-extended telomerase RNA in PABPN1-deficient cells relative to control cells (Figure 2B, F2+R1 and F2+R2; compare lanes 2 and 3 to lane 1). No robust signal was detected in the absence of reverse transcription (lanes 4–6), indicating that the observed amplifications were not due to the presence of residual genomic DNA. Notably, the use of a forward primer located upstream of mature hTR sequences (Figure 2A, see F1 primer) did not result in the detection of hTR 3′ extensions in PABPN1-depleted cells (Figure 2B, see F1+R1 and F1+R2). This result indicates that the 3′-extended telomerase RNA species detected in cells deficient for PABPN1 derive from transcription events that were initiated at the *hTR* promoter, rather than the consequence of defective transcription termination events that were initiated upstream of the *hTR* gene. The qRT-PCR analysis using primer sets complementary to sequences located downstream of the *hTR* gene confirmed the accumulation of 3′-extended telomerase RNA in PABPN1-depleted cells (Figure 2C).

Next, we sought to obtain evidence for the accumulation of 3′-extended telomerase RNA using an approach that did not depend on PCR amplification. Northern blot analyses of total RNA prepared from PABPN1-depleted cells using strand-specific RNA probes complementary to sequences downstream of mature hTR did not result in the detection of a clear signal,

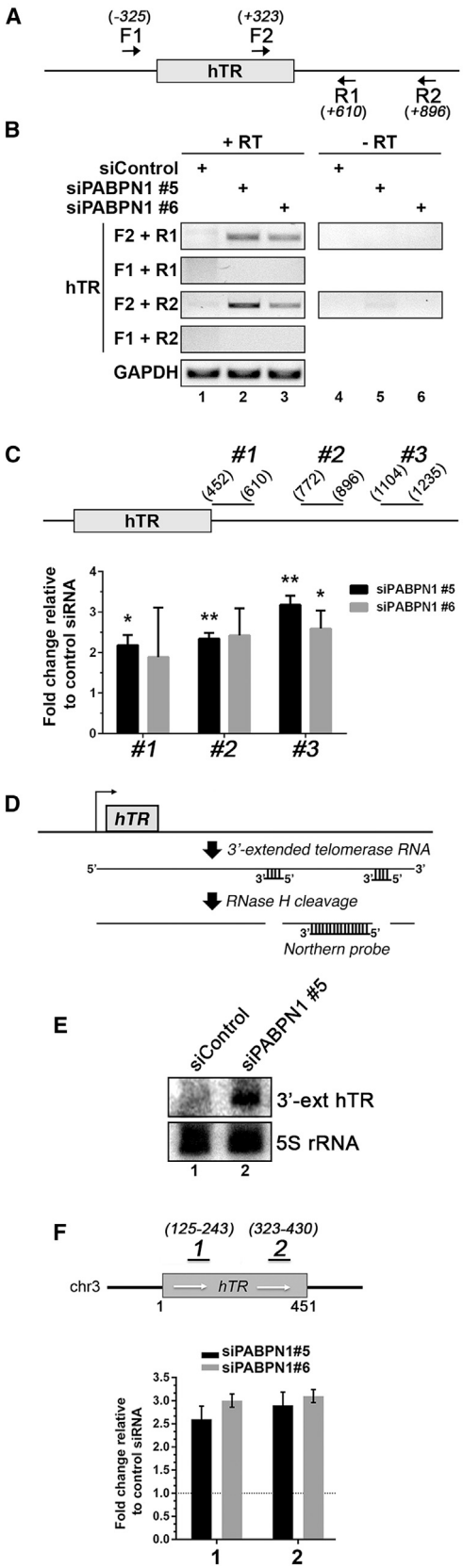

Figure 2. Accumulation of 3′-Extended and Polyadenylated Telomerase RNA in PABPN1-Deficient Cells

(A) Schematic of hTR-specific primers used to analyze hTR 3′ extenstions by RT-PCR is shown.

(B) Total RNA prepared from PABPN1-depleted (lanes 2 and 3) and control (lane 1) HeLa cells was reverse transcribed (+RT, lanes 1–3) into cDNA and analyzed for hTR 3′ extensions by PCR using the indicated combination of forward and reverse primers. Primers specific for *GAPDH* were used as internal PCR amplification control.

(C) qRT-PCR analysis of hTR 3′ extensions using RNA from PABPN1-depleted and control cells. Three independent regions downstream of the hTR gene were analyzed, as demonstrated on the schematic above the graph. Data were normalized to the 28S rRNA and expressed relative to cells treated with control siRNA. Data and error bars represent the mean and SD from three independent experiments (**$p < 0.01$ and *$p < 0.05$, Student's t test).

(D and E) Schematic of the RNase H cleavage assay used to detect 3′ extensions of the telomerase RNA. Total RNA prepared from PABPN1-depleted and control cells was treated with RNase H in the presence of DNA oligonucleotides complementary to sequences located downstream of the annotated hTR 3′ end (D). The 3′-extended (3′-ext) hTR was detected using a strand-specific riboprobe complementary to the RNase H-cleaved product. The 5S rRNA was used as a loading control (E).

(F) Total RNA from PABPN1-depleted and control cells was reverse transcribed using an oligo(dT) primer and analyzed by qPCR using two independent hTR-specific regions (see schematic), as demonstrated on the schematic above the graph. Data were normalized to the PABPC1 mRNA and expressed relative to cells treated with control siRNA. Data and error bars represent the mean and SD from three independent experiments.

suggesting heterogeneity in 3′ end distribution. Because 3′-extended telomerase RNA appeared to have heterogeneous 3′ ends, we designed an RNase H assay that would cleave the heterogeneous population of 3′-extended hTR molecules into a discrete 180-nt cleavage product (Figure 2D). Analysis of RNase H cleavage reactions by northern blotting detected a single 180-nt product in PABPN1-depleted cells (Figure 2E, lane 2); yet, this cleavage product was barely detectable in control cells (lane 1). These results indicate that a deficiency in PABPN1 leads to the accumulation of telomerase RNA with genome-encoded 3′ extensions.

Recently, RNA ligase-mediated rapid amplification of cDNA ends (RLM-RACE) coupled to deep sequencing was used to analyze the 3′ end status of various noncoding RNAs, including the human telomerase RNA (Goldfarb and Cech, 2013). Surprisingly, it was found that ~30% of hTR molecules include oligo(A) addition at the 3′ end. To examine whether polyadenylated telomerase RNA accumulates in PABPN1-deficient cells, we used an oligo(dT) primer to reverse transcribe total RNA prepared from PABPN1-deficient and control cells, and we analyzed the resulting cDNAs by qPCR using two independent hTR-specific regions. As can be seen in Figure 2F, a deficiency in PABPN1 resulted in an ~3-fold increase in the levels of polyadenylated telomerase RNA. We conclude that polyadenylated versions of the human telomerase RNA accumulate in cells deficient for PABPN1.

PABPN1 Interacts with Polyadenylated Telomerase RNA and Associates with hTERT and Dyskerin in an RNA-Dependent Manner

The aforementioned results showing reduced levels of hTR together with the accumulation of polyadenylated telomerase

RNA in PABPN1-deficient cells suggest a role for PABPN1 in hTR 3′ end maturation. To address whether PABPN1 is directly involved in hTR synthesis, we asked whether PABPN1 is bound to polyadenylated telomerase RNAs. For this, we used HEK293 cells that stably express a Flag-tagged version of PABPN1 at levels similar to endogenous PABPN1 (Figure S2A). Extracts from this stable cell line were subjected to anti-Flag affinity purification and analyzed by oligo(dT)-primed qRT-PCR using primers positioned at the 5′ end of hTR (see region 1 in Figure 2F). We also analyzed immunoprecipitates prepared from control cell lines, which recovered only background levels of polyadenylated hTR relative to Flag-PABPN1 (Figure S2B). Given the specific association between PABPN1 and polyadenylated hTR, we next analyzed the global distribution of hTR 3′ ends associated to PABPN1 by RLM-RACE coupled to high-throughout sequencing. In parallel, we analyzed the 3′ end distribution of hTR associated to Flag-tagged versions of hTERT and Dyskerin. In total, we obtained 2,716,342; 3,152,013; and 3,077,395 hTR-specific reads for the PABPN1, hTERT, and Dyskerin purifications, respectively.

Given that our focus was oligoadenylated versions of hTR, only reads with at least three consecutive non-genomic adenosines ($\geq$3) adjacent to genome-encoded hTR termini were analyzed. We also excluded reads with hTR termini upstream of the annotated 3′ end, as these truncated forms likely correspond to degradation products. We found that the majority of polyadenylated telomerase RNA recovered in the PABPN1, hTERT, and Dyskerin purifications had poly(A) tails starting immediately after the annotated hTR 3′ end (Figure 3A). However, a greater proportion of poly(A) tails were found on genome-encoded 3′ extensions in the PABPN1-bound fraction compared to the population of hTR that was copurified with hTERT and DKC1 (Figure 3A, sum of the five categories with genomic extensions): 15.5% for PABPN1, 6.9% for hTERT, and 6.5% for Dyskerin. Notably, the population of polyadenylated telomerase RNA recovered with PABPN1 was significantly different in terms of poly(A) tail length compared to polyadenylated hTR retrieved in the hTERT- and Dyskerin-bound fractions (p value = 5.551e−16, Kolmogorov-Smirnov test), showing a tendency toward longer poly(A) tails in the PABPN1-bound fraction (Figure 3B). In general, we did not find any specific trend between hTR genomic addition length and poly(A) tail retention (Figure S2C). The enrichment of telomerase RNA with long poly(A) tails in the PABPN1-bound fraction is consistent with a role of PABPN1 in a maturation pathway that depends on hTR 3′ end polyadenylation. Moreover, our results indicate that fractions of hTERT and Dyskerin are associated with polyadenylated versions of hTR.

Given the association of PABPN1 and hTERT with polyadenylated versions of hTR, we examined whether PABPN1 can copurify with the telomerase catalytic subunit by analyzing immunoprecipitates prepared from extracts of HEK293 cells that expressed Flag-hTERT as well as Flag-tagged controls. As can be seen in Figure 3C, the immunoprecipitation (IP) of Flag-hTERT also pulled down endogenous PABPN1 (lane 8). In contrast, anti-Flag precipitates prepared from extracts of control cells did not copurify appreciable levels of PABPN1 (Figure 3C, lanes 5–7). Consistent with these data, the reciprocal IP of GFP-PABPN1 specifically recovered Flag-hTERT (Figure S2D). Next, we tested whether the association between PABPN1 and hTERT was dependent on RNA by treating Flag-hTERT immunoprecipitates with a cocktail of RNases. RNase treatment abolished the association between hTERT and PABPN1 (Figure 3D, compare lanes 4 and 6), suggesting that the association is mediated by the telomerase RNA. Similar results were obtained with Dyskerin. Endogenous Dyskerin specifically copurified with Flag-PABPN1 (Figure 3E, lane 4), yet the levels of PABPN1-associated Dyskerin were strongly reduced after RNase treatment (Figure 3F, compare lanes 4 and 6). To control for the lack of proteolysis during our RNase treatment, we confirmed that the direct interaction between PRMT3 and RPS2 (Bachand and Silver, 2004) was resistant to the RNase treatment (Figure S2E). We conclude that a fraction of PABPN1-bound polyadenylated telomerase RNA is associated with hTERT and Dyskerin. Because PABPN1 interacts specifically with hTR, hTERT, and Dyskerin, three known components of active human telomerase, we also examined whether catalytically active telomerase was associated with PABPN1. Eluates of Flag-PABPN1 purifications pulled down only a small percentage of telomerase activity compared to eluates prepared from Flag-hTERT purifications (Figures S2F and S2G), suggesting that PABPN1 is not a stable component of the telomerase holoenzyme but rather of a pre-telomerase complex.

The RNA Exosome Controls Human Telomerase RNA Levels

In fission yeast, Pab2 promotes the maturation of polyadenylated snoRNA precursors via the 3′–5′ exonucleolytic activity of Rrp6, whereas the core exosome (Dis3) targets defective snoRNAs for complete degradation (Larochelle et al., 2012; Lemay et al., 2010). To test the involvement of the human exosome in telomerase RNA expression, we knocked down hRRP40 (EXOSC3), a subunit of the core exosome complex, as well as the exosome-associated 3′–5′ exonuclease hRRP6 (EXOSC10). We also knocked down the evolutionarily conserved RNA helicase hMTR4 (SKIV2L2), which is part of two distinct cofactors for the human exosome: (1) the nucleolar-enriched hTRAMP polyadenylation complex (Fasken et al., 2011; Lubas et al., 2011), and (2) the nuclear exosome targeting (NEXT) complex (Lubas et al., 2011). Western blot validations confirmed robust depletion efficiencies (Figure 4A).

As can be seen in Figure 4B, depletion of hMTR4 resulted in the greatest increase in the levels of 3′-extended telomerase RNA, while siRNAs specific to the *hRRP40* mRNA resulted in an ~10-fold increase in the levels of hTR 3′ extension. Accumulation of 3′-extended hTR also was noted in hRRP6-depleted cells, but the levels were lower than those of cells deficient for hRRP40 (Figure 4B). The accumulation of 3′-extended telomerase RNA in exosome- and hMTR4-deficient cells was confirmed by RNase H cleavage assays. Consistent with the qRT-PCR data, northern analysis of RNase H cleavage reactions detected the greatest accumulation of 3′-extended telomerase RNA in hMTR4-depleted cells (Figure 4C, lane 2). A clear cleavage product also was detected in hRRP40-deficient cells (Figure 4C, lane 3). However, the RNase H cleavage assay was not sufficiently sensitive to readily detect hTR 3′ extensions in hRRP6-depleted

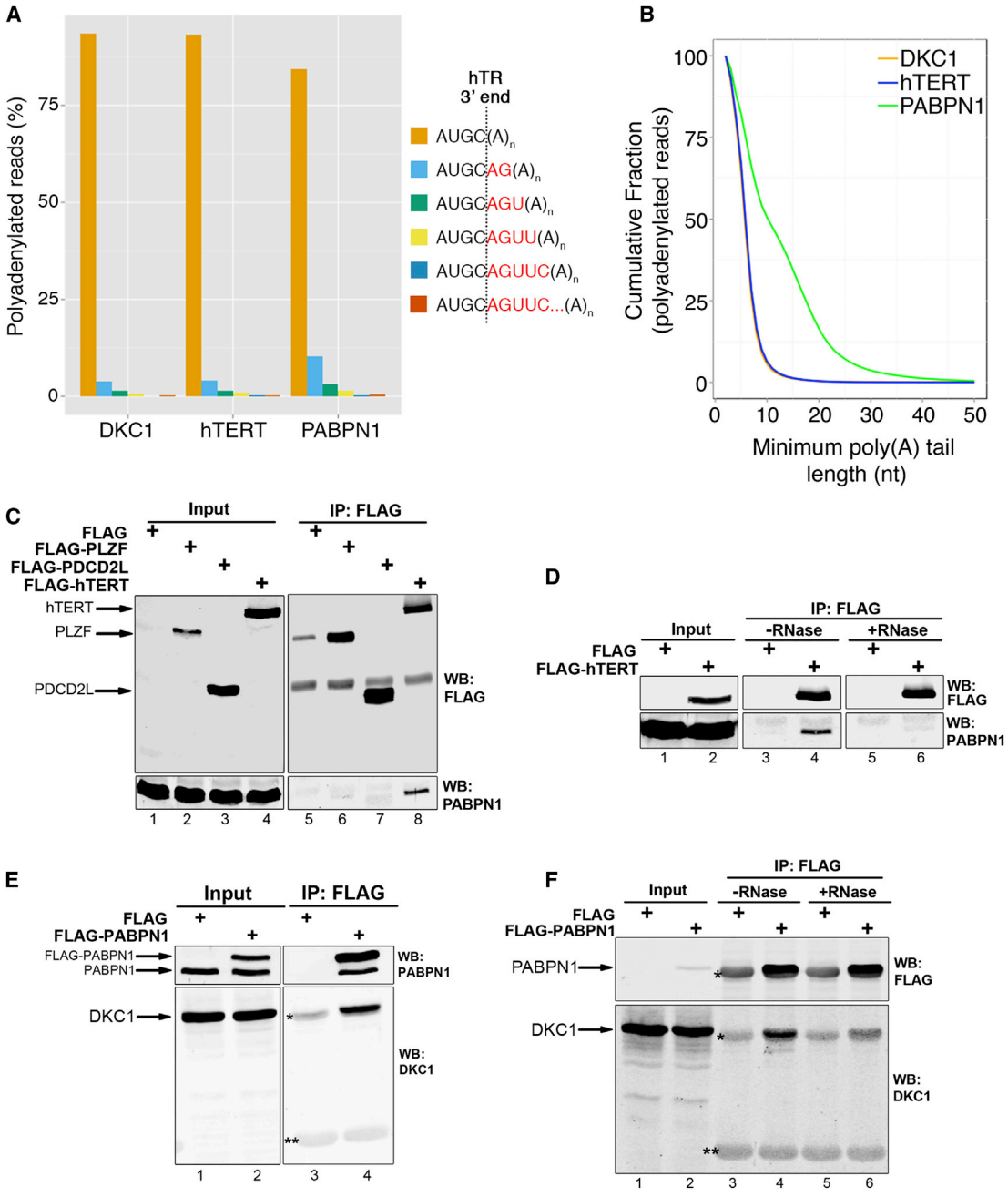

Figure 3. PABPN1 Binds to Polyadenylated hTR and Copurifies with hTERT and Dyskerin

(A) The 3′ end distribution of polyadenylated hTR associated to DKC1, hTERT, and PABPN1. The population of polyadenylated hTR was divided into six categories, where the top sequence listed is the annotated hTR 3′ end and genome-encoded extended 3′ termini are shown in red.

(B) Cumulative distribution plots comparing poly(A) tail length frequency (%) across the set of polyadenylated hTR molecules associated to DKC1, hTERT, and PABPN1 are shown.

(C) Western analysis of whole-cell extract (Input, lanes 1–4) and FLAG immunoprecipitates (IP; lanes 5–8) prepared from HEK293 cells that were previously transfected with the empty vector or constructs that expressed Flag-tagged versions of PLZF, PDCD2L, and hTERT. Western blot analysis was performed using antibodies specific to Flag (upper panel) and PABPN1 (bottom panel).

(D) Similar to (C) with the exception that anti-Flag precipitates were treated (lanes 5 and 6) or not treated (lanes 3 and 4) with a cocktail of RNases before western analysis.

(E) Western analysis of whole-cell extract (Input; lanes 1 and 2) and FLAG immunoprecipitates (IP; lanes 3 and 4) prepared from HEK293 cells that stably express Flag-PABPN1 or control vector. Western analysis was performed using antibodies specific to PABPN1 (upper panel) and DKC1 (bottom panel). Asterisks indicate the positions of denatured heavy (*) and light (**) anti-Flag IgG chains detected during the DKC1 western analysis.

(F) Similar to (E) with the exception that anti-Flag precipitates were treated (lanes 5 and 6) or not treated (lanes 3 and 4) with a cocktail of RNases before western analysis.

See also Figure S2.

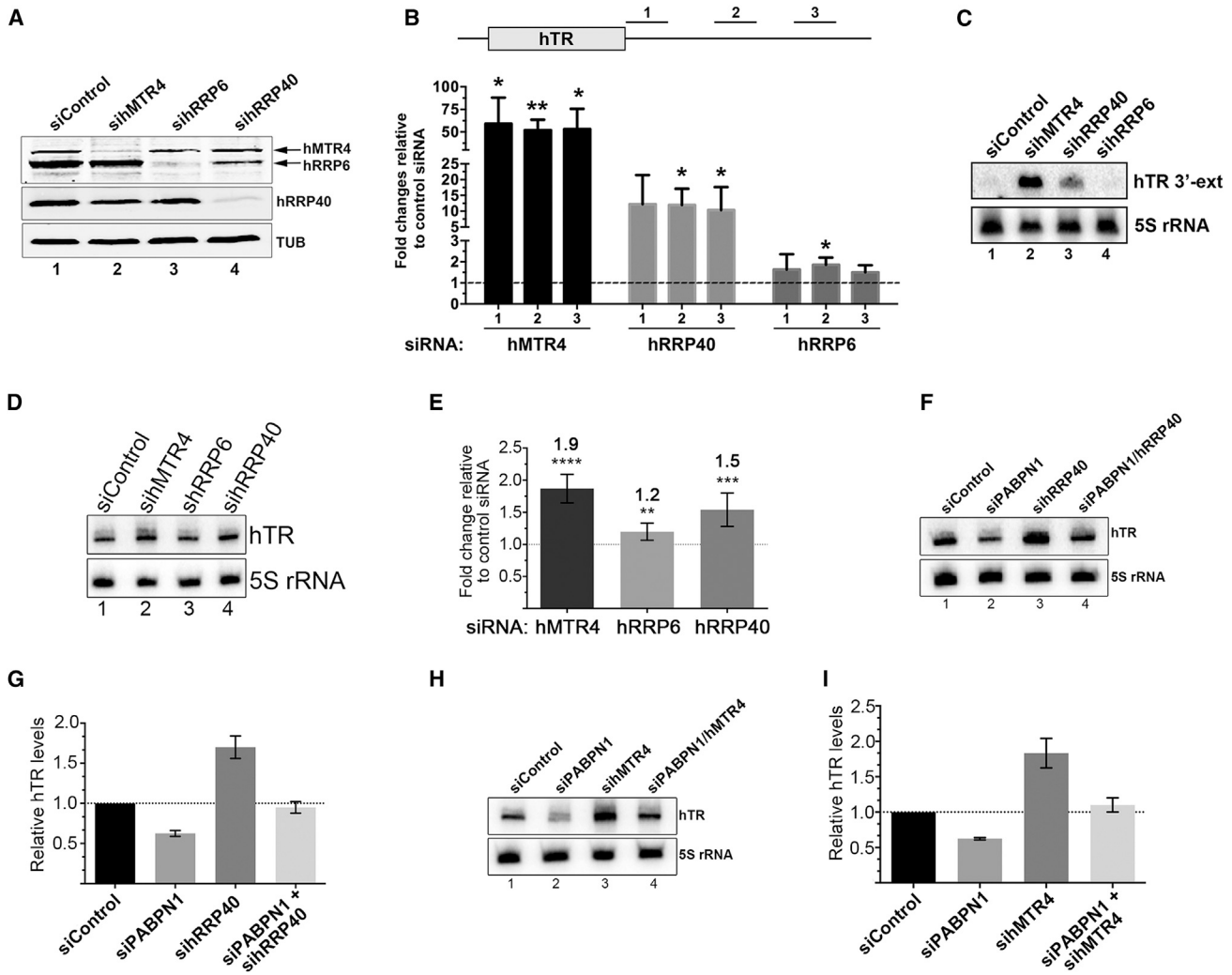

Figure 4. The Human RNA Exosome Promotes Telomerase RNA Degradation

(A) Western blot analysis shows efficient depletion of hMTR4, hRRP6, and hRRP40 from HeLa cells.

(B) qRT-PCR analysis of hTR 3′ extensions using RNA from hMTR4-, hRRP40-, and hRRP6-depleted and control cells, as described in Figure 2C. Data and error bars represent the mean and SD from four independent experiments (**$p < 0.01$ and *$p < 0.05$, Student's t test).

(C) Northern analysis of RNase H cleavage assay to detect hTR 3′ extensions (3′-ext) used RNA from hMTR4-, hRRP40-, and hRRP6-depleted cells as well as control cells.

(D) Northern blot analysis of hTR using total RNA prepared from HeLa cells treated with the indicated siRNAs. The 5S rRNA was used as a loading control.

(E) The hTR levels were normalized to the 5S rRNA and expressed relative to cells treated with control siRNA. Data and error bars represent the mean and SD from six independent experiments (****$p < 0.0001$, ***$p < 0.001$, and **$p < 0.01$, Student's t test).

(F and H) Total RNA prepared from cells treated with the indicated siRNAs was subjected to northern blot analysis using probes complementary to hTR sequence. The 5S rRNA was used as a loading control.

(G and I) The hTR levels were normalized to the 5S rRNA and expressed relative to cells treated with control siRNA. Data and error bars represent the average and SD from three independent experiments.

See also Figure S3.

cells (Figure 4C, lane 4). The greater effects seen in hMTR4-depleted cells relative to exosome subunit deficiencies are entirely consistent with data probing different exosome targets (Lubas et al., 2011), and they may be related to the pleiotropic roles of hMTR4 (Lubas et al., 2011) and/or the difficulty to efficiently deplete components of the nuclear exosome (van Dijk et al., 2007). Similarly, the smaller impact of hRRP6 depletion on hTR 3′ extensions compared to hRRP40 also agrees with previous studies of exosome targets (Lubas et al., 2011; Preker et al., 2008) and likely reflects the redundancy between hRRP6 and hDIS3 exonucleases (Tseng et al., 2015).

Next, we measured the impact of a deficiency in hMTR4 and the RNA exosome on the levels of mature hTR by northern blot analysis. In contrast to PABPN1, depletion of hMTR4, hRRP40, and hRRP6 showed increased levels of mature hTR (Figure 4D). Quantification of northern blot data from independent

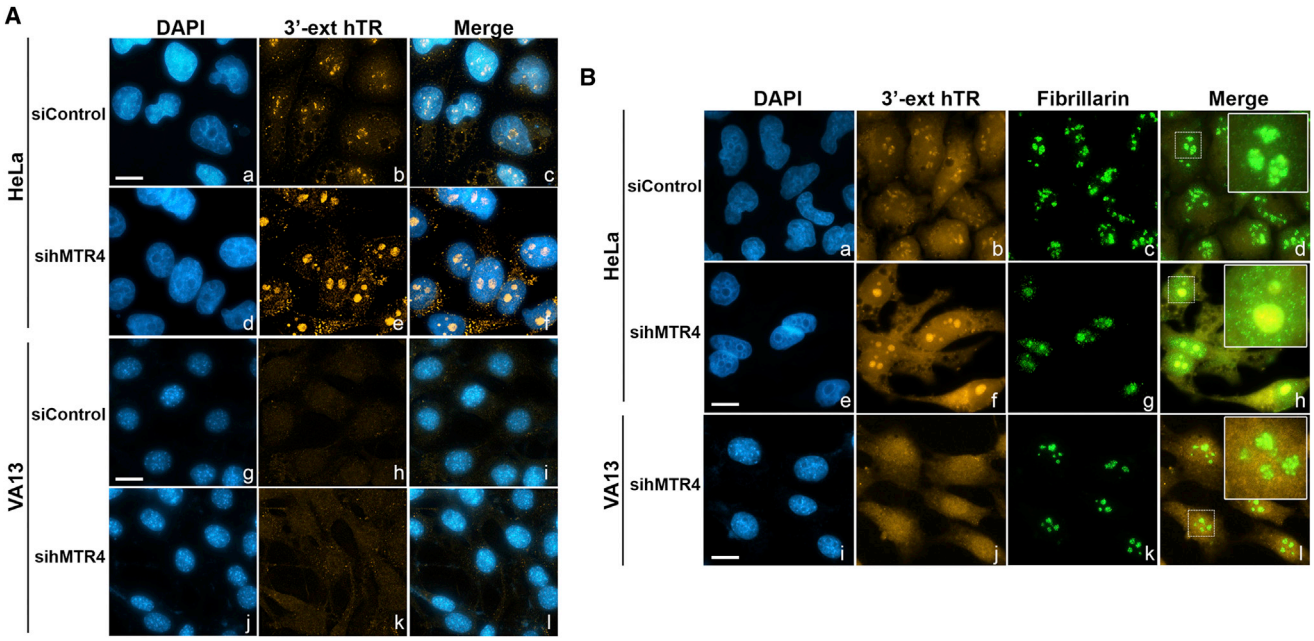

Figure 5. 3′-Extended hTR Localizes to the Nucleolus

(A) Deconvoluted images of HeLa (a–f) and VA13 (g–l) cells that were previously transfected with hMTR4-specific (d–f and j–l) or control (a–c and g–i) siRNAs were analyzed by FISH using Cy3-labeled probes for 3′-extended hTR (b, e, h, and k). DNA stained with DAPI shows the nucleus of each cell (a, d, g, and j). Scale bars, 20 μm.

(B) HeLa (a–h) and VA13 (i–l) cells that were previously transfected with hMTR4-specific (e–l) or control (a–d) siRNAs were simultaneously analyzed by FISH using Cy3-labeled probes for 3′-extended hTR (b, f, and j) and immunostaining for the nucleolar marker fibrillarin (c, g, and k). Insets (d, h, and l) show higher magnifications of nucleoli. Scale bars, 20 μm.

knockdown experiments revealed that a deficiency in hMTR4 results in an almost 2-fold increase in hTR levels (Figure 4E), whereas deficiencies in hRRP40 and hRRP6 result in 1.5- and 1.2-fold increases, respectively (Figure 4E). Interestingly, the accumulation of hTR detected in hMTR4- and hRRP40-depleted cells did not appear to affect total human telomerase activity (Figure S3). Collectively, the concomitant accumulation of both 3′-extended and mature forms of the telomerase RNA in exosome- and hMTR4-deficient cells is consistent with roles in a degradation pathway that limits hTR accumulation.

Although the aforementioned data support a role for the exosome and hMTR4 in human telomerase RNA metabolism, our results suggest that they function in a pathway that contrasts to that of PABPN1, which promotes hTR synthesis. To determine whether PABPN1 is required for the accumulation of hTR observed in hMTR4- and hRRP40-depleted cells, we analyzed hTR expression from cells in which PABPN1 was co-depleted with either hMTR4 or hRRP40. The absence of PABPN1 reproducibly suppressed the accumulation of mature hTR detected in cells deficient for hRRP40 (Figure 4F, lanes 3 and 4; Figure 4G) and hMTR4 (Figure 4H, lanes 3 and 4; Figure 4I), suggesting that PABPN1-dependent hTR maturation generally functions in an antagonistic manner to hMTR4-dependent exosome-mediated degradation.

3′-Extended Telomerase RNAs Are Enriched in Nucleoli

Analysis of telomerase RNA localization by fluorescence in situ hybridization (FISH) indicates that hTR is sequestered in Cajal bodies (CBs) for the majority of the cell cycle (Jády et al., 2004; Zhu et al., 2004). To get insight into the subcellular distribution of 3′-extended telomerase RNA, a set of 20-nt-long oligonucleotide probes was designed to specifically detect the 3′-extended form of hTR by FISH. Analysis of this set of Cy3-labeled probes in HeLa cells produced punctate signals that were mainly concentrated in the nucleus (Figure 5A, b and c). As a control, we analyzed the same FISH probes using VA13 human fibroblasts, which is a telomerase-negative cell line with undetectable levels of hTR (Bryan et al., 1997; Xi and Cech, 2014). Punctate nuclear signals were not detected in VA13 cells (Figure 5A, h and i), indicating that the nuclear signal produced in HeLa cells is specific to hTR expression. Accordingly, the signal detected with FISH probes targeting hTR 3′ extensions clearly increased in cells deficient for hMTR4 (Figure 5A, compare e and f to b and c), consistent with results obtained by qRT-PCR and RNase H assays (Figures 4B and 4C). In contrast, knockdown of hMTR4 in VA13 cells produced background signal (Figure 5A, k). These results indicate that 3′-extended telomerase RNAs mainly localize to specific regions of the nucleus.

The nuclear distribution pattern of hTR 3′ extensions detected in HeLa cells was reminiscent of a nucleolar staining, which are sites of H/ACA snoRNA maturation (Darzacq et al., 2006). To test this possibility and further characterize the localization of 3′-extended hTR in the nucleus, the FISH analysis was combined with an immunostaining procedure for endogenous fibrillarin, which is a nucleolar marker protein. Comparison of the different

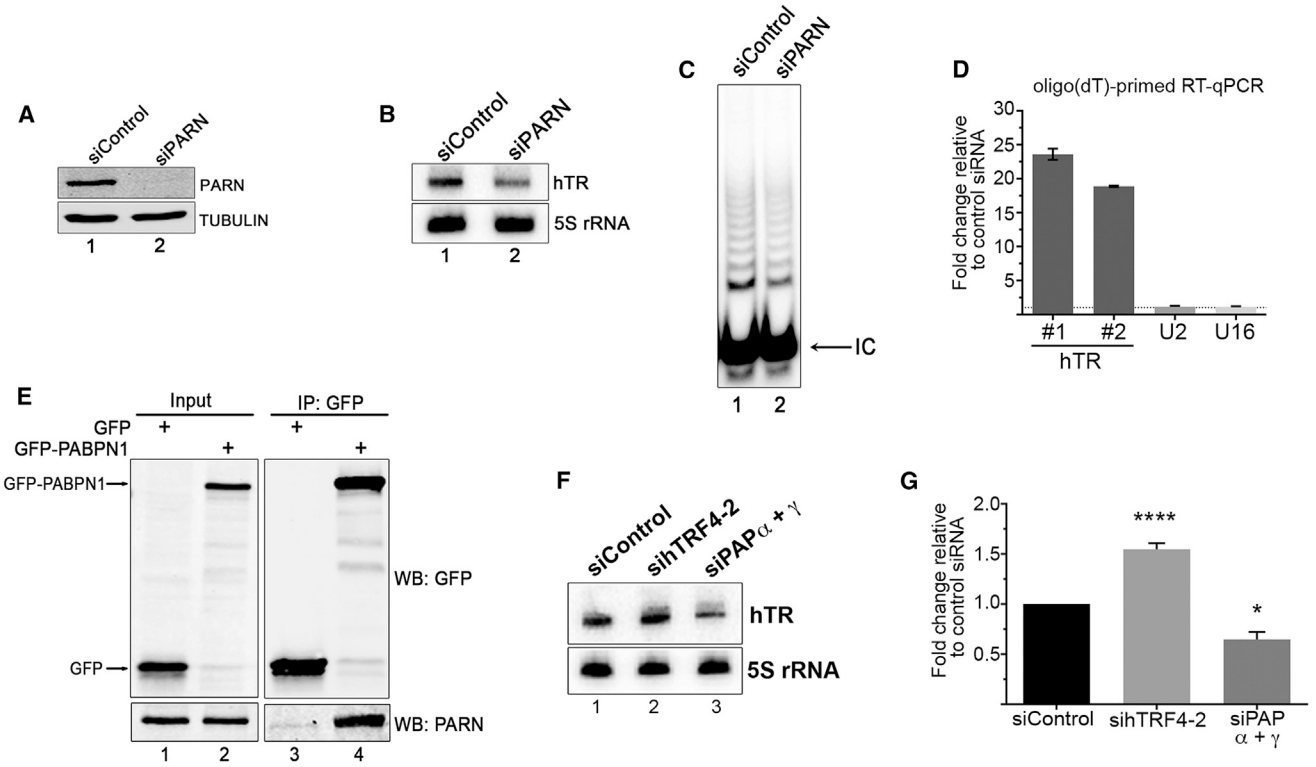

Figure 6. Poly(A)-Specific RNase and PAPs Are Required for hTR Synthesis

(A) Western blot validation shows depletion of PARN from HeLa cells.

(B) Northern blot analysis of hTR using total RNA prepared from PARN-depleted and control cells. The 5S rRNA was used as a loading control.

(C) TRAP assays used extracts prepared from HeLa cells that were previously treated with PARN-specific and control siRNAs. IC, internal PCR control.

(D) qRT-PCR analysis of oligo(dT)-primed cDNA prepared using RNA from PARN-depleted and control cells. Two independent hTR-specific regions (one and two, see Figure 2F) as well as U2 and U16 RNAs were analyzed. Data were normalized to the PABPC1 mRNA and expressed relative to cells treated with control siRNA. Data and error bars represent the mean and SD from three independent experiments.

(E) Western analysis of total extracts (Input, lanes 1 and 2) and anti-GFP immunoprecipitates (IP, lanes 3 and 4) from cells that stably express GFP and GFP-PABPN1 is shown.

(F) Northern blot analysis of hTR using total RNA prepared from HeLa cells treated with the indicated siRNAs. The 5S rRNA was used as a loading control.

(G) The hTR levels were normalized to the 5S rRNA and expressed relative to cells treated with control siRNA (****$p < 0.0001$ and *$p < 0.05$, Student's t test). Data and error bars represent the average and SD from three independent experiments.

See also Figure S4.

staining methods showed that 3′-extended telomerase RNAs were concentrated in nuclear regions that colocalized with anti-fibrillarin staining (Figure 5B, b–d). Such a specific colocalization between hTR 3′-extended species and fibrillarin also was detected in hMTR4-depleted HeLa cells (Figure 5B, e–h). In contrast, VA13 cells did not show Cy3-labeled nuclear staining that specifically colocalized with fibrillarin (Figure 5B, i–l). From these FISH experiments, we conclude that 3′-extended telomerase RNAs primarily localize to the nucleolus.

The polyA-Specific RNase Is Required for hTR Synthesis

The increased level of mature hTR detected in exosome-deficient cells, which contrasts to the hTR deficiency seen in PABPN1-depleted cells, suggested a role for the RNA exosome in telomerase RNP surveillance rather than in 3′ end trimming of polyadenylated hTR precursors. Interestingly, two recent studies reported telomere dysfunction in cells with mutations in the *PARN* gene (Stuart et al., 2015; Tummala et al., 2015), which codes for a poly(A)-specific RNase (PARN) that has been shown to be involved in the 3′ end trimming of intronic H/ACA box snoRNAs (Berndt et al., 2012). To examine whether PARN is involved in hTR 3′ end maturation, we depleted *PARN* mRNAs from HeLa cells. After validating PARN depletion by western blotting (Figure 6A), we analyzed hTR levels by northern blot using total RNA prepared from cells treated with PARN-specific and control siRNAs. PARN depletion resulted in decreased levels of telomerase RNA (Figure 6B; quantification in Figure S4A) and reduced telomerase activity (Figure 6C; quantification in Figure S4B) compared to control cells. Similar results were obtained by depleting PARN in HEK293 cells (Figures S4C and S4D). Cells deficient for PARN also accumulated polyadenylated versions of hTR, as determined by oligo(dT)-primed RT-qPCR (Figure 6D). As controls, polyadenylated versions of U2 snRNA and C/D box U16 snoRNA were not affected by a deficiency in PARN (Figure 6D), consistent with results showing that C/D box snoRNAs are not PARN substrates (Berndt et al., 2012). The shared

phenotypes resulting from PARN and PABPN1 loss of functions, including reduced levels of hTR and telomerase activity, as well as telomere shortening, suggested a functional relationship between these two proteins in hTR 3′ end maturation. Accordingly, comparison of PABPN1 and PARN single depletions to PABPN1/PARN double depletions showed similar levels of hTR reduction (Figures S4E–S4G), suggesting that both proteins function in a common pathway such that when cells are deficient for PABPN1, depletion of PARN exerts no further defects in hTR maturation. Consistent with the idea that PABPN1 and PARN function in a common pathway of telomerase RNA maturation, endogenous PARN was specifically enriched after affinity purification of GFP-PABPN1 relative to a control GFP purification (Figure 6E, lanes 3 and 4). The association between PABPN1 and PARN was found to be partially resistant to RNases (Figure S4H). Together, these data suggest that PARN is required for PABPN1-dependent processing of polyadenylated telomerase RNA.

We also set out to characterize the complex responsible for hTR polyadenylation. Two major polyadenylation machineries are responsible for RNA oligoadenylation in the nucleus of human cells: (1) the canonical PAPs that catalyze mRNA polyadenylation (Shi and Manley, 2015), and (2) the hTRAMP complex (Fasken et al., 2011; Lubas et al., 2011) that targets transcripts for decay by the nuclear exosome. Via RNAi-mediated gene silencing, we depleted the catalytic subunit of these two polyadenylation complexes: hTRF4-2 (PAPD5) for the hTRAMP complex and both PAPα and PAPγ for the canonical polyadenylation machinery. Consistent with roles in promoting hTR polyadenylation, oligo(dT)-primed qRT-PCR analysis of hTRF4-2- and PAPα/PAPγ-deficient cells both resulted in lower levels of polyadenylated hTR compared to cells treated with control siRNAs (Figure S4I). However, contrasting effects were observed at the levels of mature hTR. Depletion of hTRF4-2 resulted in increased levels of mature hTR (Figure 6F, lane 2; Figure 6G), a result consistent with the increased hTR accumulation observed after depletion of hMTR4 (Figures 4D and 4E), which forms the hTRAMP complex via associations with hTRF4-2 and the RNA-binding proteins ZCCHC7 (Fasken et al., 2011; Lubas et al., 2011). In contrast, co-depletion of PAPα and PAPγ elicited a telomerase RNA deficiency (Figure 6F, lane 3; Figure 6G). These results suggest that polyadenylation by the canonical PAPs promotes hTR maturation, whereas hTRAMP-dependent polyadenylation triggers telomerase RNA decay.

DISCUSSION

In this study, we identified an unexpected role for the nuclear poly(A)-binding protein PABPN1 in the biogenesis of hTR and in telomere maintenance, disclosing a polyadenylation-dependent step in the 3′ end maturation of hTR. We also found evidence that the RNA exosome functions antagonistically to PABPN1-dependent hTR maturation, thereby limiting telomerase RNA accumulation. In addition to providing novel insights into the mechanism of telomerase RNA 3′ end processing, our results establish a critical role for RNA polyadenylation in telomerase-mediated telomere maintenance.

A Polyadenylation-Dependent Pathway Promotes 3′ End Maturation of the hTR

While evidence for oligoadenylated telomerase RNA was reported previously (Goldfarb and Cech, 2013), the functional relevance of hTR polyadenylation had remained unknown. Here we show that a deficiency in PABPN1 results in reduced levels of mature hTR together with the accumulation of polyadenylated versions of the telomerase RNA, providing strong evidence for the role of PABPN1 in a 3′ end maturation pathway that leads to the production of mature telomerase RNA. The functional importance of PABPN1 in hTR production is further demonstrated by a deficiency in telomere maintenance in PABPN1-depleted cells (Figure 1). Because RNA sequencing (RNA-seq) analysis of poly(A)$^+$ RNA from PABPN1-depleted cells indicates that close to 96% of detected mRNAs are normally expressed (Beaulieu et al., 2012), the negative impact of a PABPN1 deficiency on hTR levels, telomerase activity, and telomere length is likely to reflect the direct role of PABPN1 in telomerase RNA maturation. Accordingly, the expressions of *hTERT*, *DKC1*, *NHP2*, *NOP10*, *NAF1*, *GAR1*, and *RUVBL1/L2* mRNAs are not affected in cells deficient for PABPN1 (Beaulieu et al., 2012). Importantly, the direct role of PABPN1 in the polyadenylation-dependent maturation of hTR is supported by (1) the enrichment of telomerase RNA with long poly(A) tails in the PABPN1-bound fraction (Figure 3B), and (2) the copurification of hTERT and Dyskerin with PABPN1 (Figure 3). These findings, together with our previous work on *S. pombe* snoRNA 3′ end processing (Larochelle et al., 2012; Lemay et al., 2010), support the existence of an evolutionarily conserved role for Pab2/PABPN1 in the maturation of independently transcribed H/ACA box RNAs.

The nature of the PAP activity associated with PABPN1-dependent maturation of hTR also appears to be conserved. Indeed, whereas the canonical nuclear PAP Pla1 is associated to Pab2-dependent snoRNA maturation in *S. pombe* (Lemay et al., 2010), Cid14, the catalytic subunit of the fission yeast TRAMP polyadenylation complex, promotes the turnover of nonproductive snoRNPs (Larochelle et al., 2012). Accordingly, mature snoRNAs accumulate in *cid14 S. pombe* mutants, analogous to the increased levels of mature hTR detected after the depletion of the human Cid14 homolog hTRF4-2 (Figure 6). In contrast, the targeted knockdown of the canonical human PAPs, PAPα and PAPγ, resulted in hTR deficiency (Figure 6), consistent with a pathway leading to mature telomerase RNA. Although we cannot exclude the possibility that the hTR deficiency observed in PAPα/PAPγ-depleted cells is the consequence of secondary effects, the fact that almost half of the polyadenylated telomerase RNA associated to PABPN1 have poly(A) tails longer than 15 nt (Figure 3B) is consistent with the involvement of canonical PAPs in PABPN1-dependent maturation. In contrast, the distribution of RNAs polyadenylated by TRAMP peaks at four to five adenosines (Schmidt and Butler, 2013).

Our study identified the poly(A)-specific RNase PARN as an exoribonuclease that functions with PABPN1 to promote hTR 3′ end processing. This conclusion is based on the following clearly detectable effects of PARN depletion (Figure 6): reduced hTR accumulation and a robust increase in polyadenylated forms of the telomerase RNA. Consistent with our findings, a role for PARN in the 3′ end maturation of intronic H/ACA box

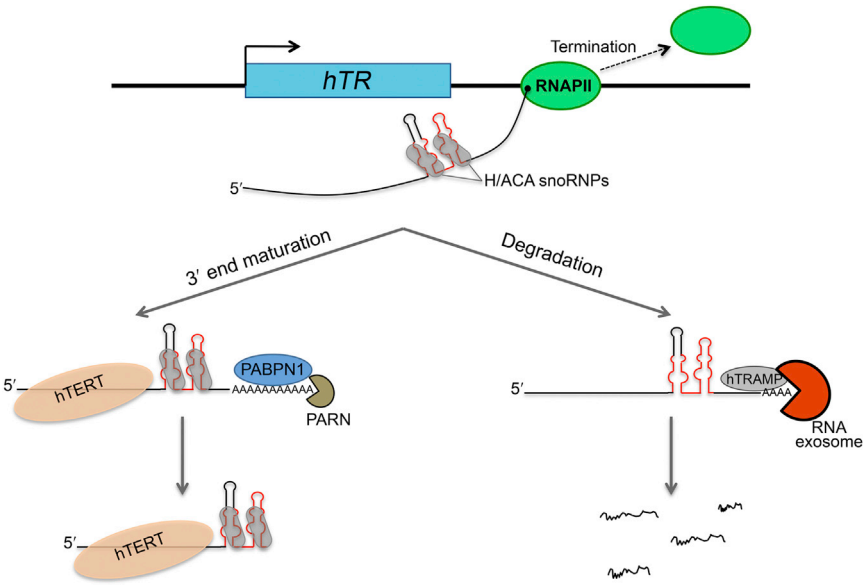

Figure 7. Model for Polyadenylation-Dependent Telomerase RNA Maturation

Transcription of nascent hTR by RNA polymerase II (Pol II) is associated with the co-transcriptional recruitment of H/ACA RNP assembly factors (H/ACA snoRNPs). Termination of hTR transcription is coupled to two antagonistic pathways that actively compete for nascent hTR precursors: PABPN1/PARN-dependent 3′ end maturation and hTRAMP/exosome-dependent decay. The equilibrium between decay and maturation of telomerase RNA precursors thus controls hTR expression.

snoRNAs has been demonstrated previously, whereby knockdown of PARN resulted in the accumulation of polyadenylated versions of SNORA63 and SNORA65 together with reduced levels of their mature forms (Berndt et al., 2012). Quite remarkably, two recent studies in fact documented *PARN* mutations in human disorders linked to telomere dysfunctions, dyskeratosis congenita (Tummala et al., 2015) and idiopathic pulmonary fibrosis (Stuart et al., 2015), further supporting the role of PARN in hTR synthesis. The ability of PABPN1 to stimulate PAP-dependent poly(A) tail synthesis (Bresson and Conrad, 2013; Wahle, 1991) may promote the generation of a high-affinity substrate for PARN, which is a poly(A)-specific 3′–5′ exonuclease (Körner and Wahle, 1997). Physical interactions between PABPN1 and PARN (Figure 6) also may contribute to recruiting PARN at the 3′ end of polyadenylated hTR precursors. The identification of PARN and PABPN1, two proteins with high specificity for poly(A) tails, as factors promoting hTR synthesis strongly supports a polyadenylation-dependent 3′ end maturation pathway for the human telomerase RNA.

Our results support a model in which mature hTR is produced via 3′ end trimming of polyadenylated precursors in a process that requires PABPN1 and PARN (Figure 7). According to this model, the polyadenylated telomerase RNA accumulating in PABPN1- and PARN-deficient cells corresponds to pre-hTR stalled or delayed in 3′ end processing, thereby resulting in reduced hTR accumulation. To explain the accumulation of mature hTR in cells deficient for the human TRAMP complex (knockdown of hMTR4 and hTRF4-2), we propose that hTRAMP-dependent polyadenylation promotes a degradation pathway that actively competes with PABPN1/PARN-dependent telomerase RNA maturation (Figure 7). Consistent with this model, hTR accumulation also was observed upon knockdown of hRRP40 and hRRP6 (Figure 4), components of the human RNA exosome, which is known to be stimulated by the polyadenylation activity of the hTRAMP complex (Lubas et al., 2011). The increased accumulation of hTR in exosome/hTRAMP-deficient cells supports the view that a fraction of telomerase RNA produced in normal cells is constantly discarded before entering functional pathways, suggesting that kinetic competition between degradation and maturation determines the efficiency and accuracy of hTR processing (Figure 7). Although it remains possible that TRAMP/exosome-dependent decay also influences the turnover of mature hTR independently of hTR precursors, the fact that 3′-extended telomerase RNA accumulated in exosome- and hTRAMP-deficient cells (Figures 4B and 4C) argues that the nuclear exosome does not act exclusively on mature hTR.

The connection between the two types of hTR 3′ extension reported here, the near-mature polyadenylated versions of hTR and the longer 3′-extended species, remains to be determined and likely will be enlightened by elucidating the mechanism of hTR transcription termination. One possible scenario is the influence of a transcription termination pathway that promotes termination of Pol II transcription at the annotated hTR 3′ end, or a few nucleotides downstream, as reported for NNS-dependent termination of independently transcribed yeast snoRNAs (Kim et al., 2006; Steinmetz et al., 2001) and the *S. cerevisiae* telomerase RNA (Noël et al., 2012). Such transcription termination would be coupled to two antagonistic pathways that actively compete for nascent hTR precursors (Figure 7): PABPN1/PARN-dependent maturation and hTRAMP/exosome-dependent decay. In this scenario, the long and heterogeneous 3′-extended hTR species are non-functional products resulting from read-through transcription and targeted for RNA decay via exosome-dependent surveillance mechanisms (Lemay et al., 2014; West et al., 2006). However, as redundant transcription termination pathways can converge for the production of functional noncoding RNAs (Grzechnik and Kufel, 2008; Lemay et al., 2010; Noël et al., 2012), it remains possible that the long 3′-extended hTR species may be processed sporadically into mature hTR.

Nucleolar Localization of 3′-Extended hTR

Previous localization studies in immortalized human cell lines indicate that the telomerase RNA accumulates in a nuclear structure (Cajal Body; CB) and that hTR localization to the CB is

important for telomere maintenance by telomerase (Cristofari et al., 2007; Jády et al., 2004; Theimer et al., 2007; Zhu et al., 2004). In contrast, little is known about the subnuclear localization of the maturation steps that occur before routing of hTR to the CB and whether only 3′ end-processed hTR accumulates in the CB. Our localization analyses of 3′-extended telomerase RNA by FISH suggest that part of hTR 3′ end processing takes place in the nucleolus. This conclusion is supported by previous localization studies that used ectopically expressed hTR in telomerase-negative VA13 cells, which showed that mutations in the CB-targeting signal results in the accumulation of processed hTR in nucleoli (Theimer et al., 2007), arguing for nucleolar 3′ end processing steps prior to CB localization. Similarly, depletion of TCAB1, which targets hTR to the CB, results in the accumulation of hTR in the nucleolus (Freund et al., 2014). The detection of endogenous 3′-extended hTR in the nucleolus (Figure 5) is also consistent with the nucleolar localization of the human TRAMP complex and of exosome subunits (Lubas et al., 2011). Remaining to be determined is the localization of near-mature polyadenylated versions of hTR, as it is currently challenging to distinguish these polyadenylated forms from mature hTR by FISH. However, as immunostaining studies suggest that both PARN and PABPN1 include nucleolar targeting elements (Berndt et al., 2012; Calado et al., 2000), it is tempting to speculate that final trimming of polyadenylated telomerase RNA precursors also occurs in the nucleolus.

Although hTR biogenesis can occur in the absence of hTERT (Yi et al., 1999), the mechanism and localization of hTERT-hTR assembly remain poorly understood. The identification of polyadenylated versions of hTR in affinity-purified hTERT preparations, together with the RNase-sensitive copurification of PABPN1 and hTERT, suggests that a fraction of polyadenylated hTR precursors include hTERT during terminal 3′ end maturation steps (Figure 7). Although the functional significance of these associations remains to be determined, the idea that hTERT recruitment occurs prior to terminal hTR 3′ end maturation is consistent with results showing that hTERT expression can promote hTR accumulation (Yi et al., 1999).

In summary, our study identified key factors critical for the 3′ end maturation of the independently transcribed hTR, and, by doing so, it provides evidence for the unsuspected role of RNA polyadenylation in telomerase-mediated telomere maintenance. As mutations in *PARN* have been linked to human diseases of telomere dysfunction (Stuart et al., 2015; Tummala et al., 2015), our findings suggest that mutations in *PABPN1* also may be found in patients with dyskeratosis congenita, aplastic anemia, and pulmonary fibrosis, as the causal mutations in many families afflicted by these syndromes of telomere shortening remain to be determined.

EXPERIMENTAL PROCEDURES

Cell Culture and Transfections

HeLa and HEK293 cells were cultured in DMEM while WI38-VA13 cells (ATCC) were grown in Eagle's minimal essential medium (EMEM). Stable cell lines that conditionally induced GFP- and Flag-tagged fusions were maintained in DMEM containing 10% tetracycline-free fetal bovine serum (FBS), Hygromycine (75 μg/ml), and Blasticidin (15 μg/ml). Expression from the tetracycline-sensitive promoter was induced using 500 ng/ml doxycycline. The siRNAs were transfected at 20 nM using lipofectamine 2000 (Life Technologies) and maintained for 72–96 hr. Sequences of siRNAs used in this study are listed in Table S1.

Protein Analyses

Preparation of cell lysates for western blotting and IPs was as previously described (Beaulieu et al., 2012). For IPs with RNase treatment, the beads were incubated 30 min at 25°C with 7.5 U RNase A and 300 U RNase T1. Immunoblotting signals were detected using an Odyssey infrared imaging system (LI-COR Biosciences) and quantified by Image Studio version 3.1 software. A list of antibodies used in this study is provided in the Supplemental Experimental Procedures.

RNA Analyses

Total RNA was extracted with TRIzol (Life Technologies) and analyzed by northern blotting and qRT-PCR, as described previously (Beaulieu et al., 2012). RNase H cleavage assays were previously described (Lemay et al., 2014) and are explained in detail in the Supplemental Experimental Procedures. Conditions for the semiquantitative RT-PCR analyses (Figure 2) and the sequences of probes used for northern blotting are described in the Supplemental Experimental Procedures. Primers are listed in Table S2.

TRAP

TRAP assays from total cell extracts were as described previously (Bachand et al., 2002).

Analysis of hTR 3′ End

RNA co-immunoprecipitation (RIP) assays and extraction of RNA from beads were as previously described (Bergeron et al., 2015). Preparation of hTR-specific libraries using immunoprecipitated RNA was based on the RNA ligase-mediated 3′ RACE approach described by Goldfarb and Cech (2013), using the primers listed in Table S3. Barcoded libraries were combined and analyzed on an Illumina MiSeq instrument. Data analysis was based on a custom python script, which is described in detail in the Supplemental Experimental Procedures.

TRF Assay

TRF analyses were done as previously described (Kimura et al., 2010) with minor modifications. Briefly, 3 μg genomic DNA was digested with *Rsa*I and *Hin*fI and resolved on 0.5% agarose gels. The gel was transferred onto nylon membranes, cross-linked, and incubated with ^{32}P-labeled telomere-specific probe $(CCCTAA)_3$ at 55°C overnight. The radioactive signal was detected and quantified using a Typhoon Trio instrument. Mean TRF lengths were analyzed using TeloTool (Göhring et al., 2014).

FISH and Immunofluorescence Detection

The FISH signals were detected using Cy3-labeled *Stellaris* probes (Biosearch Technologies), as recommended per the manufacturer's instructions. A detailed description can be found in the Supplemental Experimental Procedures.

ACCESSION NUMBERS

The accession number for the RNA-seq data reported in this paper is GEO: GSE74186.

SUPPLEMENTAL INFORMATION

Supplemental Information includes Supplemental Experimental Procedures, four figures, and three tables and can be found with this article online at http://dx.doi.org/10.1016/j.celrep.2015.11.003.

ACKNOWLEDGMENTS

We thank P. Baumann for sharing unpublished data; B. Lemieux for help with the TRF analysis; F. Dragon for the Flag-Dyskerin construct; and

C. Autexier, P. Chartrand, and R. Wellinger for comments on the manuscript. This work was supported by the Canadian Institutes of Health Research grant MOP-106595 to F.B. and by a postdoctoral fellowship from the Centre de Recherche du Centre Hospitalier Universitaire de Sherbrooke (CRCHUS) to D.N. F.B. is a Canada Research Chair in the Quality Control of Gene Expression.

Received: June 4, 2015
Revised: October 2, 2015
Accepted: October 29, 2015
Published: November 25, 2015

REFERENCES

Artandi, S.E., and DePinho, R.A. (2010). Telomeres and telomerase in cancer. Carcinogenesis *31*, 9–18.

Bachand, F., and Autexier, C. (2001). Functional regions of human telomerase reverse transcriptase and human telomerase RNA required for telomerase activity and RNA-protein interactions. Mol. Cell. Biol. *21*, 1888–1897.

Bachand, F., and Silver, P.A. (2004). PRMT3 is a ribosomal protein methyltransferase that affects the cellular levels of ribosomal subunits. EMBO J. *23*, 2641–2650.

Bachand, F., Boisvert, F.M., Côté, J., Richard, S., and Autexier, C. (2002). The product of the survival of motor neuron (SMN) gene is a human telomerase-associated protein. Mol. Biol. Cell *13*, 3192–3202.

Beattie, T.L., Zhou, W., Robinson, M.O., and Harrington, L. (1998). Reconstitution of human telomerase activity in vitro. Curr. Biol. *8*, 177–180.

Beaulieu, Y.B., Kleinman, C.L., Landry-Voyer, A.M., Majewski, J., and Bachand, F. (2012). Polyadenylation-dependent control of long noncoding RNA expression by the poly(A)-binding protein nuclear 1. PLoS Genet. *8*, e1003078.

Bergeron, D., Pal, G., Beaulieu, Y.B., Chabot, B., and Bachand, F. (2015). Regulated Intron Retention and Nuclear Pre-mRNA Decay Contribute to PABPN1 Autoregulation. Mol. Cell. Biol. *35*, 2503–2517.

Berndt, H., Harnisch, C., Rammelt, C., Stöhr, N., Zirkel, A., Dohm, J.C., Himmelbauer, H., Tavanez, J.P., Hüttelmaier, S., and Wahle, E. (2012). Maturation of mammalian H/ACA box snoRNAs: PAPD5-dependent adenylation and PARN-dependent trimming. RNA *18*, 958–972.

Bresson, S.M., and Conrad, N.K. (2013). The human nuclear poly(a)-binding protein promotes RNA hyperadenylation and decay. PLoS Genet. *9*, e1003893.

Bryan, T.M., Marusic, L., Bacchetti, S., Namba, M., and Reddel, R.R. (1997). The telomere lengthening mechanism in telomerase-negative immortal human cells does not involve the telomerase RNA subunit. Hum. Mol. Genet. *6*, 921–926.

Calado, A., Kutay, U., Kühn, U., Wahle, E., and Carmo-Fonseca, M. (2000). Deciphering the cellular pathway for transport of poly(A)-binding protein II. RNA *6*, 245–256.

Chlebowski, A., Lubas, M., Jensen, T.H., and Dziembowski, A. (2013). RNA decay machines: the exosome. Biochim. Biophys. Acta *1829*, 552–560.

Cristofari, G., Adolf, E., Reichenbach, P., Sikora, K., Terns, R.M., Terns, M.P., and Lingner, J. (2007). Human telomerase RNA accumulation in Cajal bodies facilitates telomerase recruitment to telomeres and telomere elongation. Mol. Cell *27*, 882–889.

Darzacq, X., Kittur, N., Roy, S., Shav-Tal, Y., Singer, R.H., and Meier, U.T. (2006). Stepwise RNP assembly at the site of H/ACA RNA transcription in human cells. J. Cell Biol. *173*, 207–218.

Dieci, G., Preti, M., and Montanini, B. (2009). Eukaryotic snoRNAs: a paradigm for gene expression flexibility. Genomics *94*, 83–88.

Egan, E.D., and Collins, K. (2012). Biogenesis of telomerase ribonucleoproteins. RNA *18*, 1747–1759.

Fasken, M.B., Leung, S.W., Banerjee, A., Kodani, M.O., Chavez, R., Bowman, E.A., Purohit, M.K., Rubinson, M.E., Rubinson, E.H., and Corbett, A.H. (2011). Air1 zinc knuckles 4 and 5 and a conserved IWRXY motif are critical for the function and integrity of the Trf4/5-Air1/2-Mtr4 polyadenylation (TRAMP) RNA quality control complex. J. Biol. Chem. *286*, 37429–37445.

Freund, A., Zhong, F.L., Venteicher, A.S., Meng, Z., Veenstra, T.D., Frydman, J., and Artandi, S.E. (2014). Proteostatic control of telomerase function through TRiC-mediated folding of TCAB1. Cell *159*, 1389–1403.

Göhring, J., Fulcher, N., Jacak, J., and Riha, K. (2014). TeloTool: a new tool for telomere length measurement from terminal restriction fragment analysis with improved probe intensity correction. Nucleic Acids Res. *42*, e21.

Goldfarb, K.C., and Cech, T.R. (2013). 3′ terminal diversity of MRP RNA and other human noncoding RNAs revealed by deep sequencing. BMC Mol. Biol. *14*, 23.

Grzechnik, P., and Kufel, J. (2008). Polyadenylation linked to transcription termination directs the processing of snoRNA precursors in yeast. Mol. Cell *32*, 247–258.

Jády, B.E., Bertrand, E., and Kiss, T. (2004). Human telomerase RNA and box H/ACA scaRNAs share a common Cajal body-specific localization signal. J. Cell Biol. *164*, 647–652.

Kim, N.W., Piatyszek, M.A., Prowse, K.R., Harley, C.B., West, M.D., Ho, P.L., Coviello, G.M., Wright, W.E., Weinrich, S.L., and Shay, J.W. (1994). Specific association of human telomerase activity with immortal cells and cancer. Science *266*, 2011–2015.

Kim, M., Vasiljeva, L., Rando, O.J., Zhelkovsky, A., Moore, C., and Buratowski, S. (2006). Distinct pathways for snoRNA and mRNA termination. Mol. Cell *24*, 723–734.

Kimura, M., Stone, R.C., Hunt, S.C., Skurnick, J., Lu, X., Cao, X., Harley, C.B., and Aviv, A. (2010). Measurement of telomere length by the Southern blot analysis of terminal restriction fragment lengths. Nat. Protoc. *5*, 1596–1607.

Kiss, T., Fayet-Lebaron, E., and Jády, B.E. (2010). Box H/ACA small ribonucleoproteins. Mol. Cell *37*, 597–606.

Körner, C.G., and Wahle, E. (1997). Poly(A) tail shortening by a mammalian poly(A)-specific 3′-exoribonuclease. J. Biol. Chem. *272*, 10448–10456.

Larochelle, M., Lemay, J.F., and Bachand, F. (2012). The THO complex cooperates with the nuclear RNA surveillance machinery to control small nucleolar RNA expression. Nucleic Acids Res. *40*, 10240–10253.

Lemay, J.F., D'Amours, A., Lemieux, C., Lackner, D.H., St-Sauveur, V.G., Bähler, J., and Bachand, F. (2010). The nuclear poly(A)-binding protein interacts with the exosome to promote synthesis of noncoding small nucleolar RNAs. Mol. Cell *37*, 34–45.

Lemay, J.F., Larochelle, M., Marguerat, S., Atkinson, S., Bähler, J., and Bachand, F. (2014). The RNA exosome promotes transcription termination of backtracked RNA polymerase II. Nat. Struct. Mol. Biol. *21*, 919–926.

Lubas, M., Christensen, M.S., Kristiansen, M.S., Domanski, M., Falkenby, L.G., Lykke-Andersen, S., Andersen, J.S., Dziembowski, A., and Jensen, T.H. (2011). Interaction profiling identifies the human nuclear exosome targeting complex. Mol. Cell *43*, 624–637.

Mitchell, J.R., Cheng, J., and Collins, K. (1999a). A box H/ACA small nucleolar RNA-like domain at the human telomerase RNA 3′ end. Mol. Cell. Biol. *19*, 567–576.

Mitchell, J.R., Wood, E., and Collins, K. (1999b). A telomerase component is defective in the human disease dyskeratosis congenita. Nature *402*, 551–555.

Noël, J.F., Larose, S., Abou Elela, S., and Wellinger, R.J. (2012). Budding yeast telomerase RNA transcription termination is dictated by the Nrd1/Nab3 noncoding RNA termination pathway. Nucleic Acids Res. *40*, 5625–5636.

Porrua, O., and Libri, D. (2015). Transcription termination and the control of the transcriptome: why, where and how to stop. Nat. Rev. Mol. Cell Biol. *16*, 190–202.

Preker, P., Nielsen, J., Kammler, S., Lykke-Andersen, S., Christensen, M.S., Mapendano, C.K., Schierup, M.H., and Jensen, T.H. (2008). RNA exosome depletion reveals transcription upstream of active human promoters. Science *322*, 1851–1854.

Schmidt, K., and Butler, J.S. (2013). Nuclear RNA surveillance: role of TRAMP in controlling exosome specificity. Wiley Interdiscip. Rev. RNA *4*, 217–231.

Shi, Y., and Manley, J.L. (2015). The end of the message: multiple protein-RNA interactions define the mRNA polyadenylation site. Genes Dev. *29*, 889–897.

Steinmetz, E.J., Conrad, N.K., Brow, D.A., and Corden, J.L. (2001). RNA-binding protein Nrd1 directs poly(A)-independent 3′-end formation of RNA polymerase II transcripts. Nature *413*, 327–331.

Stuart, B.D., Choi, J., Zaidi, S., Xing, C., Holohan, B., Chen, R., Choi, M., Dharwadkar, P., Torres, F., Girod, C.E., et al. (2015). Exome sequencing links mutations in PARN and RTEL1 with familial pulmonary fibrosis and telomere shortening. Nat. Genet. *47*, 512–517.

Theimer, C.A., Jády, B.E., Chim, N., Richard, P., Breece, K.E., Kiss, T., and Feigon, J. (2007). Structural and functional characterization of human telomerase RNA processing and cajal body localization signals. Mol. Cell *27*, 869–881.

Tseng, C.-K., Wang, H.-F., Burns, A.M., Schroeder, M.R., Gaspari, M., and Baumann, P. (2015). Human telomerase RNA processing and quality control. Cell Rep. *13*, this issue, 2232–2243.

Tudek, A., Porrua, O., Kabzinski, T., Lidschreiber, M., Kubicek, K., Fortova, A., Lacroute, F., Vanacova, S., Cramer, P., Stefl, R., and Libri, D. (2014). Molecular basis for coordinating transcription termination with noncoding RNA degradation. Mol. Cell *55*, 467–481.

Tummala, H., Walne, A., Collopy, L., Cardoso, S., de la Fuente, J., Lawson, S., Powell, J., Cooper, N., Foster, A., Mohammed, S., et al. (2015). Poly(A)-specific ribonuclease deficiency impacts telomere biology and causes dyskeratosis congenita. J. Clin. Invest. *125*, 2151–2160.

van Dijk, E.L., Schilders, G., and Pruijn, G.J.M. (2007). Human cell growth requires a functional cytoplasmic exosome, which is involved in various mRNA decay pathways. RNA *13*, 1027–1035.

Vulliamy, T., Beswick, R., Kirwan, M., Marrone, A., Digweed, M., Walne, A., and Dokal, I. (2008). Mutations in the telomerase component NHP2 cause the premature ageing syndrome dyskeratosis congenita. Proc. Natl. Acad. Sci. USA *105*, 8073–8078.

Wahle, E. (1991). A novel poly(A)-binding protein acts as a specificity factor in the second phase of messenger RNA polyadenylation. Cell *66*, 759–768.

Webb, C.J., Wu, Y., and Zakian, V.A. (2013). DNA repair at telomeres: keeping the ends intact. Cold Spring Harb. Perspect. Biol. *5*, a012666.

West, S., Gromak, N., Norbury, C.J., and Proudfoot, N.J. (2006). Adenylation and exosome-mediated degradation of cotranscriptionally cleaved pre-messenger RNA in human cells. Mol. Cell *21*, 437–443.

Xi, L., and Cech, T.R. (2014). Inventory of telomerase components in human cells reveals multiple subpopulations of hTR and hTERT. Nucleic Acids Res. *42*, 8565–8577.

Yi, X., Tesmer, V.M., Savre-Train, I., Shay, J.W., and Wright, W.E. (1999). Both transcriptional and posttranscriptional mechanisms regulate human telomerase template RNA levels. Mol. Cell. Biol. *19*, 3989–3997.

Zhu, Y., Tomlinson, R.L., Lukowiak, A.A., Terns, R.M., and Terns, M.P. (2004). Telomerase RNA accumulates in Cajal bodies in human cancer cells. Mol. Biol. Cell *15*, 81–90.